Development 129, 2293-2302 (2002)
Printed in Great Britain © The Company of Biologists Limited 2002
DEV14525

DEVELOPMENT AND DISEASE

A complex syndrome of left-right axis, central nervous system and axial skeleton defects in *Zic3* mutant mice

Smita M. Purandare[1,*], Stephanie M. Ware[2,*], Kin Ming Kwan[3], Marinella Gebbia[1], Maria Teresa Bassi[1], Jian Min Deng[3], Hannes Vogel[1,4], Richard R. Behringer[3], John W. Belmont[2] and Brett Casey[1,4,†]

[1]Department of Pathology, Baylor College of Medicine, Houston, TX 77030, USA
[2]Department of Molecular and Human Genetics, Baylor College of Medicine, Houston, TX 77030, USA
[3]Department of Molecular Genetics, University of Texas M.D. Anderson Cancer Center, Houston, TX 77030, USA
[4]Department of Pathology, Texas Children's Hospital, Houston, TX 77030, USA
*These authors contributed equally to this work
[†]Author for correspondence (e-mail: bcasey@cw.bc.ca)

Accepted 17 December 2001

SUMMARY

X-linked heterotaxy (HTX1) is a rare developmental disorder characterized by disturbances in embryonic laterality and other midline developmental field defects. HTX1 results from mutations in *ZIC3*, a member of the GLI transcription factor superfamily. A targeted deletion of the murine *Zic3* locus has been created to investigate its function and interactions with other molecular components of the left-right axis pathway. Embryonic lethality is seen in approximately 50% of null mice with an additional 30% lethality in the perinatal period. Null embryos have defects in turning, cardiac development and neural tube closure. Malformations in live born null mice include complex congenital heart defects, pulmonary reversal or isomerism, CNS defects and vertebral/rib anomalies. Investigation of *nodal* expression in *Zic3*-deficient mice indicates that, although *nodal* is initially expressed symmetrically in the node, there is failure to maintain expression and to shift to asymmetric expression. Subsequent *nodal* and *Pitx2* expression in the lateral plate mesoderm in these mice is randomized, indicating that *Zic3* acts upstream of these genes in the determination of left-right asymmetry. The phenotype of these mice correctly models the defects found in human HTX1 and indicates an important role for *Zic3* in both left-right and axial patterning.

Key words: Mouse, *Zic3*, CNS, Left-right asymmetry

INTRODUCTION

The failure to establish midline body pattern and left-right asymmetry properly is an important cause of congenital malformations. These defects are associated with considerable morbidity and mortality secondary to complex congenital heart defects (CHD), immune dysfunction caused by abnormalities of spleen position or number, gut malrotation, and midline central nervous system (CNS) defects. *ZIC3* was the first gene identified to have a causal role in defects of human laterality. Loss-of-function mutations in *ZIC3* cause HTX1, which results in heterotaxy or situs ambiguus, the aberrant positioning of internal organs with respect to each other and the left-right (LR) axis. Carrier females who are heterozygous for a *ZIC3* mutation are clinically unaffected although a subset has situs inversus, the mirror image reversal of internal anatomy (Casey et al., 1993; Gebbia et al., 1997).

The molecular pathways required for correct LR axis specification and formation have been examined in different model organisms including *Xenopus*, chick, zebrafish and mouse (reviewed by Harvey, 1998; Burdine and Schier, 2000; Capdevila et al., 2000; Casey and Hackett, 2000). Pathways of asymmetric gene expression resulting in a cascade of lateralized signals that specify morphological asymmetry have been elucidated. This asymmetric gene expression is initiated at the node, or organizer, and occurs well before the first morphological sign of asymmetry, the rightward looping of the embryonic heart tube. These pathways appear to be conserved across species although the function of individual genes in the generation of LR asymmetry may be species specific.

There are at least three major processes involved in establishment of the LR axis: (1) node-dependent symmetry breaking; (2) establishment of the embryonic midline (notochord and ventral floorplate); and (3) *nodal*-dependent signaling in the left lateral plate mesoderm (LPM). Failure in any of these processes will result in disturbances of laterality, including the complete reversal of left-right anatomy (situs inversus) or randomization of organ position (situs ambiguus). Generally, situs inversus is believed to arise as a result of an early event in which either the specification of asymmetry or orientation of the LR axis with respect to anteroposterior and dorsoventral axes is disrupted. Examples

include mouse mutants *iv/iv* (Hummel and Chapman, 1959), which is caused by deletion of left-right dynein, *lrd* (Supp et al., 1997; Supp et al., 1999), *Kif3a* (Marszalek et al., 1999; Takeda et al., 1999), *Kif3b* (Nonaka et al., 1999) and hepatocyte nuclear factor/forkhead homolog 4 (*hfh-4*) (Chen et al., 1998), all of which have abnormal node ciliary function or structure. *inv* mutants, in whom the gene product has an unknown function, also show situs inversus (Yokoyama et al., 1993; Mochizuki et al., 1998). Situs ambiguus is believed to result from failure to maintain asymmetric expression of genes involved in the *nodal*-dependent signaling pathway. This final common pathway, which appears to be conserved across species, is initiated with the expression of *nodal* in the perinodal region (Collignon et al., 1996; Lowe et al., 1996). This is followed by the expression of *nodal* and *lefty2* (Meno et al., 1996; Meno et al., 1999), both TGFβ family members, and *Pitx2*, a homeobox transcription factor, in the left LPM. *Pitx2* expression appears to be the most downstream gene in this cascade and is expressed asymmetrically in the LPM as well as in developing organs including the heart and visceral progenitors (Logan et al., 1998; Piedra et al., 1998; Ryan et al., 1998; Yoshioka et al., 1998; Campione et al., 1999; Lin et al., 1999). Although it is clear from individuals with HTX1 that *ZIC3* plays a role in formation and/or specification of the left-right axis, its position within this molecular cascade is not known. The finding of both situs ambiguus and situs inversus in these individuals is unusual and suggests that *Zic3* may play roles at multiple steps within the LR axis hierarchy.

The murine Zic gene was initially identified as a zinc-finger protein expressed in granule cells throughout the development of the cerebellum (Aruga et al., 1994). Further analysis in chick confirmed the role of *Zic1* and *Zic3* in the developing cerebellum (Lin and Cepko, 1998). Currently, four paralogous *Zic* family members have been described, all of which show conservation of zinc-finger motifs that place ZIC proteins within the GLI transcription factor superfamily (Aruga et al., 1996a; Aruga et al., 1996b). The expression pattern of *Zic3* is suggestive of a role in body pattern formation (Nagai et al., 1997). In *Xenopus*, overexpression of *Zic3* induces proneural genes as well as neural crest markers (Nakata et al., 1997). Further studies in *Xenopus* have suggested that *Zic3* acts upstream of *nodal* in the signaling cascade of LR asymmetry (Kitaguchi et al., 2000). Other Zic family members are also known to have an effect on neural development and embryonic patterning, although no situs abnormalities have been described. Individuals with *ZIC2* mutations have holoprosencephaly (Brown et al., 1998). A mouse model in which *Zic2* functions as a hypomorphic allele shows a number of neural defects including holoprosencephaly, spina bifida, neurulation delay and delay in neural crest development (Nagai et al., 2000). *Xenopus Zic5* (orthologous to murine and human *Zic4*) is also important for neural crest development (Nakata et al., 2000), whereas *Zic1* appears to play an important role in skeletal patterning (Aruga et al., 1999) and cerebellar development (Aruga et al., 1998).

To address the role of *Zic3* in body pattern formation and in left-right asymmetry, we have generated *Zic3* null mice. Deletion of murine *Zic3* leads to complex congenital heart disease, disturbances of laterality, neural tube defects and vertebral and rib defects, including partial homeotic transformations of the axial skeleton. These defects indicate that *Zic3* plays an important role in both axial midline development and LR patterning. Furthermore, our results indicate that *Zic3* is involved in the maintenance of *nodal* expression and is important both for LR axis specification and maintenance of lateralized signaling. Taken together, these results suggest a role for *Zic3* in both left-right and anterior-posterior axis formation.

MATERIALS AND METHODS

Gene targeting vector construction

The mouse *Zic3* locus was cloned by screening a mouse strain 129/SvEv genomic library. The targeting vector (Fig. 1A) was constructed using a 2.6 kb *Eco*RI-*Not*I fragment comprising the 5′ end of the *Zic3* gene that extends 138 bp downstream of the translation initiation site, and a 3.9 kb *Cla*I-*Eco*RI fragment comprising the 3′ end of the gene, starting 311 bp downstream of the translation termination site. An IRES-lacZ-pA cassette followed by a PGKneobpA neomycin resistance expression cassette flanked by loxP sites (provided by Maki Wakamiya) was inserted between the two regions of *Zic3* homology. A MC1tkpA herpes simplex virus thymidine kinase expression cassette was added to the 3′ arm of homology to enrich for homologous recombinants by negative selection with 1-2-deoxy-2-fluoro-b-D-arabinofuranosyl-S-iodouracil (FIAU) (Mansour et al., 1988).

Generation and genotyping of *Zic3* mutant mice

The targeting vector was linearized at a unique *Sal*I site outside the region of sequence homology and introduced into AB-1 embryonic stem (ES) cells as described (Behringer et al., 1994; Hogan et al., 1994). 386 G418/FIAU-resistant ES cell clones were initially screened by *Bam*HI digestion and hybridized with a unique 3′ probe external to the region of vector homology. Expected sizes were 10.5 kb and 7.5 kb for the wild-type and targeted allele, respectively (data not shown). Six correctly targeted clones were identified. ES cells carrying the disrupted *Zic3* allele were injected into C57Bl/6J (B6) blastocysts, and one ES cell clone was found to be capable of contributing to the germline of mouse chimeras. Mice were genotyped by Southern blot analysis using a *Sac*I-*Xba*I fragment in the 5′ region of the gene (Fig. 1A). The expected sizes for the fragments were 3.2 kb for the wild-type and 5.8 kb for the targeted allele (Fig. 1B). Embryos were genotyped by multiplex PCR using the following primers: 5′ *Zic3* TGC AGG CAT GGG ATT GAA TCC; 3′ *Zic3* AAG AGC AAG TAG CTA GGA GGC; 5′ *Sry* TGA CTG GGA TGC AGT AGT TC; 3′ *Sry* TGT GCT AGA GAG AAA CCC TG; 5′ *lacZ* AAC TTA ATC GCC TTG CAG CA; 3′ *lacZ* GTA ACC GTG CAT CTG CCA GT. Expected product sizes were 386 bp for *Zic3*, 240 bp for *Sry* and 218 bp for *lacZ*. All primers were used in the same reaction with an annealing temperature of 58°C.

Expression analysis

Whole-mount in situ hybridization was performed using a modification of the protocol described (Wilkinson, 1992), using Blocking Reagent (Boehringer Mannheim). Probes were labeled using a DIG RNA Labeling kit (Boehringer Mannheim). A *Zic3* probe spanning 471 bp in the 3′ region of the gene was generated using PCR. The primers used for PCR were F 5′-TCTAGATTC-CTTACAATGTCAGT-3′ and R 5′-AAGAAGCACTTTAACCA-TGAG-3′. Mouse embryos were processed to visualize β-galactosidase (β-gal) activity by X-gal staining (Hogan et al., 1994).

Skeletal preparations

Embryos or neonates were harvested and staining was performed as described previously (Kochhar, 1973) using 0.015% Alcian Blue 8GX followed by 1%KOH/0.015% Alizarin Red. The skeletons were cleared in 1% KOH/20% glycerol for several days and stored in a 1:1 mixture of glycerol and 95% ethanol.

RESULTS

Generation of *Zic3*-null mice

To examine the role of *Zic3* in mouse development, the *Zic3*-coding region was deleted and replaced with a *lacZ* reporter gene in mouse ES cells (Fig. 1A,B). Because *Zic3* is located on the X chromosome, deletion in male ES cells should generate *Zic3* null cell lines. Interestingly, all of the resulting male chimeras generated with these *Zic3* null ES cell lines had tail kinks (data not shown), suggesting a role in axial development (see below).

To document that embryonic *Zic3* expression was ablated by the deletion of the *Zic3*-coding region, whole-mount in situ hybridization was performed on wild type and –/Y 9.0 days post coitum (dpc) embryos. *Zic3* expression was readily detected in the CNS, tailbud and somites of the wild-type embryo but not in the –/Y mutant embryo, demonstrating that the targeted mutation had eliminated *Zic3* expression (Fig. 1C, D).

Zic3 null mice exhibit embryonic and postnatal lethality

Female heterozygotes derived from crosses of male chimeras with B6 mice were bred with either B6 or outbred Swiss males, and their progeny (n=217) were genotyped at 3 weeks of age (Table 1). Departure from the expected mutant to wild-type ratio indicated significant lethality in the *Zic3* null males that is more dramatic on the B6/129 mixed genetic background (0.26 viability versus 0.46). Furthermore, no live-born –/Y males were recovered from crosses on the 129/SvEv inbred background (data not shown), indicating that the penetrance of the *Zic3* null allele is sensitive to genetic background differences.

All viable –/Y males, regardless of genetic background, and ~40% (17/44) of the +/– females had 'kinked' tails (Fig. 1E). This malformation was usually less severe in the females than in the males. These observations suggest that a lack of *Zic3* causes tail abnormalities. Indeed, *Zic3* has recently been found to reside within a microdeletion on the X chromosome in the classic mouse mutation *bent tail* (*Bn*) (Carrel et al., 2000; Klootwijk et al., 2000). The variability of the tail phenotype in the heterozygous females is likely to be due to X chromosome inactivation. In support of this idea, X-gal stained *Zic3* heterozygous female embryos show mosaic β-gal activity in the CNS (Fig. 1F), suggesting that the *lacZ* knock-in allele can serve as a reporter of X chromosome activation status.

Zic3 null males were mated to heterozygous females to evaluate prenatal lethality as well as the phenotype of null females. Table 1 shows results of these crosses at weaning age (n=155) and at specific gestational stages. Ratios of genotypes as compared with wild type are shown below each line of raw data and indicate a skewing from the expected 1:1:1:1 ratio. The ratio of null males compared with wild type was 0.20, indicating a lethality rate that corresponds well to data from the heterozygous by wild-type crosses. In both sets of crosses on the B6/129 background, there was a slight decrease in the viability of heterozygotes (ratio 0.77 and 0.81). Analyses of embryos at various gestational ages failed to show a discrete time point at which lethality occurs, suggesting that the embryonic losses may occur over an extended period of time. Comparison of the ratios of null males and females at birth and at weaning age demonstrate that significant lethality also occurs after birth, with approximately 30% of null males lost in the perinatal period. In addition, the null females appear to be less affected in utero but have a larger percentage (50%) that die after birth.

Severe developmental anomalies and laterality defects in *Zic3* null embryos

To investigate the timing and cause of prenatal lethality in *Zic3* deleted mice, embryos were harvested, genotyped and

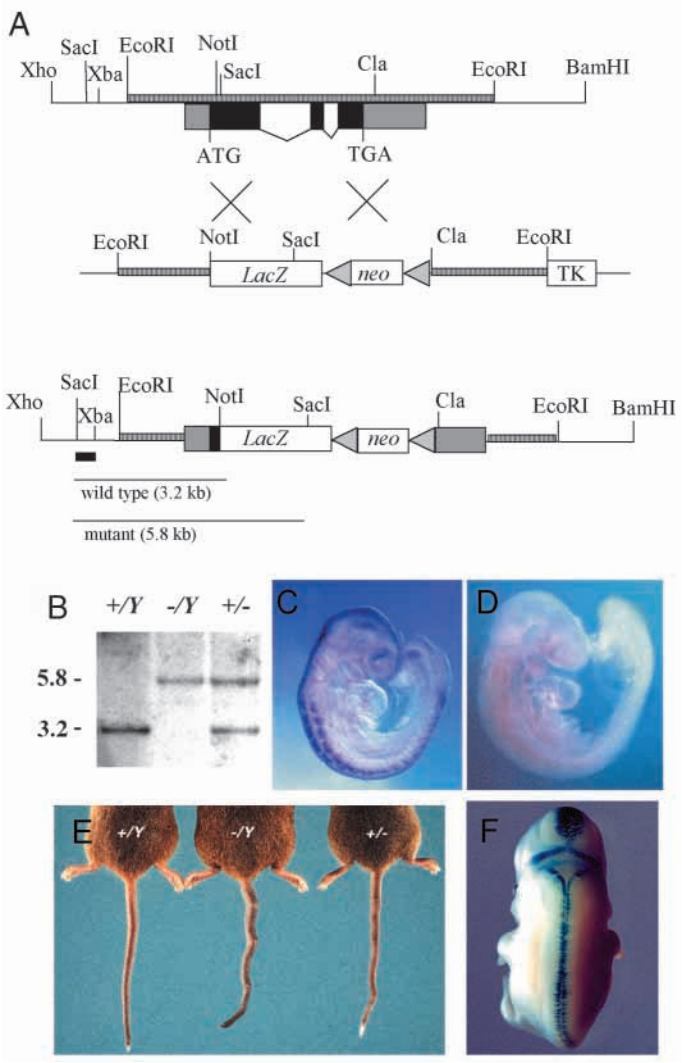

Fig. 1. Targeted disruption of *Zic3*. (A) Wild-type *Zic3* genomic locus (top), the targeting vector (middle) and targeted allele (bottom). *Zic3* exons shown with black boxes with 3′UTR and 5′UTR in gray; striped boxes indicate homology; gray triangles indicate loxP sites. (B) Southern blot analysis of tail DNA digested with *Sac*I and hybridized using an external 5′ probe. The 3.2 kb wild-type and 5.8 kb targeted alleles are shown. (C,D) Results of in situ hybridization on 17-20 somite (9 dpc) embryos using a *Zic3* probe shows the expected expression pattern in a wild-type male (C) and absence of expression (D) in a null male embryo. (E) Tail phenotype of +/Y, –/Y and +/– mutants (F) β-gal expression in the CNS of a *Zic3* heterozygous female 11.5 dpc embryo. Note that the staining of β-gal is mosaic, indicating that the targeted allele is reporting X chromosome inactivation status.

Table 1. Genotype analyses of *Zic3* mice indicating embryonic and post-natal lethality

Stage or age	Cross	Strain	Number analyzed	+/+	+/y	+/–	–/y	–/–
Adult	(+/y) × (+/–)	C57/129	107	35	36	27	9	–
Ratio				1	1	0.77	0.26	
	(+/y) × (+/–)	C57/Swiss	110	30	33	33	14	–
Ratio				1	1.1	1.1	0.46	
Adult	(–/y) × (+/–)	C57/129	155	–	68	55	16	16
Ratio					1	0.81	0.20	0.20
Embryos	(–/y) × (+/–)	C57/129						
≤10.5 dpc			43	–	17	12	7(3)	7(3)
11.5-13.5 dpc			35	–	10	12	3	10(1)
14.5-18.5 dpc			95	–	25	32	17	21
Total			173	–	52	56	27	38
Ratio					1	1.1	0.52	0.73

Numbers in parentheses represent embryos that were dead and/or resorbing at the time of dissection and are not included in totals. –, no genotype expected.

examined at varying gestational stages. As indicated in Table 1, there was not a definitive time point of lethality. Rather, the embryos appear to die at different gestational stages with a variety of defects. In the 65 *Zic3* null embryos examined, several laterality defects, including failure and delay of embryonic turning as well as abnormal direction of turning (Fig. 2A,B) were seen. Several null embryos that survived beyond the turning stage exhibited significant rotation defects manifest by abnormal thoracic and lumbar flexion and/or abnormal looping of the distal tail including the hindlimb buds (Fig. 2E-H; compare with wild type in Fig. 2C). Other laterality defects included abnormalities of heart looping and position. At 10.5 dpc, the heart is located at the midline. However, in several null embryos, the heart was positioned to the left side of the thorax (Fig. 2D,F). This was not simply a result of abnormal embryonic turning, because abnormally turned mice with midline hearts were seen as well (Fig. 2G). This aberrant positioning is similar to that noted previously in sonic hedgehog (*Shh*) deficient mice (Tsukui et al., 1999). In contrast to the *Shh*$^{-/-}$ mice, however, aberrant right lateralization of the heart was also found in a smaller number (*n*=2) of *Zic3* null embryos.

Zic3 null embryos also demonstrated CNS defects. Neural tube closure was delayed in some *Zic3* null embryos at 8.5 dpc (compare neural fold apposition in Fig. 2A with 2B). In a subset of embryos, the headfolds were not well formed (data not shown). By 9.5 dpc, neural tube defects were noted with failure of fusion present in the midbrain-hindbrain region. Several embryos with neural tube defects appeared to be dead at 10.5 and 11.5 dpc, based on lack of a heart beat (Fig. 2I). In addition, abnormalities in the size and structure of the midbrain and forebrain, including the region overlying the telencephalic vesicles (Fig. 2F), were seen. Many *Zic3* null embryos without obvious gross anatomical abnormalities nevertheless showed evidence of growth delay when compared with their wild-type littermates (data not shown). These delayed embryos were found at all time points analyzed, demonstrating that embryos had a broad range of developmental defects.

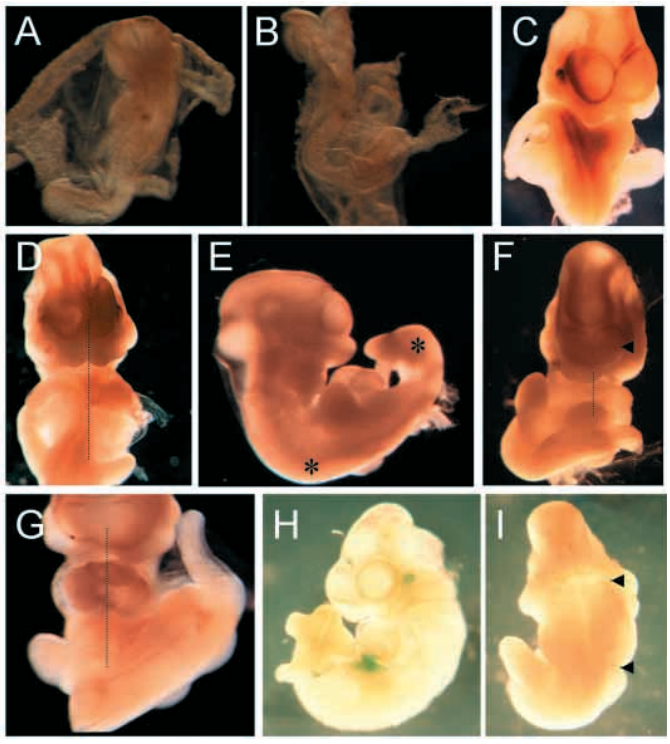

Fig. 2. *Zic3* null embryos exhibit multiple laterality defects and CNS anomalies. (A) Dorsal view of wild-type embryo at 8.5 dpc, demonstrating normal turning and apposition of the neural folds. (B) Dorsal view of a –/Y embryo at 8.5 dpc, showing abnormal turning and lack of elevation and apposition of the neural folds in the cephalic region. (C) 10.5 dpc wild-type embryo with tail turned to right of midline. (D) 10.5 dpc –/– null female with heart left of midline. (E) Right lateral view of 10.5 dpc –/– null female with abnormal turning and increased thoracic and lumbar flexion (*). (F) Ventral view of embryo in E, demonstrating left lateral position of heart and underdeveloped telencephalic vesicles lacking an obvious midline (arrowhead). (G) 10.5 dpc –/– null female with abnormal turning, midline heart positioning and abnormal cardiac looping. (H) –/Y null male at 10.5 dpc, normally turned except for distal tail including hindlimb buds. (I) Neural tube defect in –/– female harvested at 12.5 dpc; the embryo had no heartbeat and development was consistent with 10.5-11 dpc. Arrowheads indicate the margins of the neural tube defect, which extends from the midbrain-hindbrain junction to the lumbar region.

A complex syndrome of left-right axis, neural tube and axial skeleton defects

Seventy-six null and heterozygous offspring were analyzed at 17.5-18.5 dpc to investigate the causes of perinatal lethality. Internal malformations were identified at necropsy in 7 (24%)

Zic3 null (either –/Y or –/–) fetuses and in one +/– female. In addition, newborns that were either runted, in obvious distress or stillborn were analyzed. Internal malformations were identified in 25, including six female heterozygotes.

Table 2 summarizes the internal malformations, which include defects of the LR axis, CNS and axial skeleton. No differences were detected between null mice and heterozygous females, aside from the frequency of malformations. Of the 20 mice with LR malformations, only one, a heterozygous female, had situs inversus. Seventeen had heart defects, including dextro-transposition of the great arteries (most commonly), interrupted aortic arch, right aortic arch, atrial septal defect, ventricular septal defect and abnormal systemic venous connections (Fig. 3A-C). Heart anomalies in the null and heterozygous *Zic3* mice were always found in combination with other anomalies and were never found in isolation. Abnormal lung morphology included complete reversal (n=3), bilateral left-sided (both lungs unilobate, n=2) and bilateral right-sided (both lungs with four lobes, n=9) (Fig. 3D). A right-sided stomach with reversed liver lobation was seen in six mice. A spleen was identified in all affected mutants, but it was often hypoplastic (Fig. 3E,F).

Five pups obtained by Caesarian section were exencephalic, and two newborns found dead had anencephaly (Fig. 3G). One pup had a completely open spine from the cervical to the lumbar region, one had meningocoele and one had an open neural tube defect in the lumbosacral spine. All of the exencephalic brains had very similar histological abnormalities: disorganized cerebral cortex, anteriorly displaced diencephalon, disorganized basal ganglia, thalamus and hippocampus, rudimentary olfactory nerves, and absent cerebellum (Fig. 3H,I). None of these abnormalities were identified in any *Zic3* null or +/– pups with an intact skull.

Zic3 expression is detected in differentiating somites (Fig. 1C). By 10.5 dpc, *Zic3* expression is restricted to the dorsal dermamyotome and subepidermal dorsal mesenchyme (Nagai et al., 1997). Twelve mice (10 null and two heterozygous) had malformations of the axial skeleton. Almost all of the anomalies were unilateral and appeared to be posterior transformations along the anteroposterior axis (Fig. 3J-N). Vertebral abnormalities included partial duplications, partial fusions and apparent homeotic transformations. Partial rib duplications and inappropriately posterior sites of rib insertion were also identified. The sidedness of the malformations appeared to be random (five right, seven left) and there was no correlation with the sidedness of LR malformations when they were present. The only bilaterally symmetric abnormalities were the absence of one pair of ribs in two pups and partial atlanto-axial (C1-C2) fusions in the midline in four pups; these six pups also had additional, unilateral malformations of the axial skeleton.

Nodal and *Pitx2* are aberrantly regulated in *Zic3* null embryos

In recent years, a genetic hierarchy has been defined that regulates the formation of the LR axis (reviewed by Burdine and Schier, 2000; Capdevila et al., 2000; Casey and Hackett, 2000). *Zic3* expression has been examined in embryos ≤8.0 dpc by in situ hybridization of histological sections, but no asymmetrical expression was reported (Nagai et al., 1997). We obtained similar results, with symmetric expression observed in all of the embryos studied from 6.5 dpc to 10.5 dpc (data not shown). Specifically, transcripts were detected symmetrically in (but not limited to) the primitive streak and node at all stages in which these structures were present.

To examine the relationship of *Zic3* with other genes involved in LR axis specification, whole-mount in situ hybridization was performed with probes directed against *Pitx2* and *nodal*. *Pitx2* is expressed asymmetrically in the left lateral plate mesoderm beginning at the two to four somite stage and persists on the left side of the developing heart and gut through 16 dpc. *Pitx2* is currently one of the most downstream regulatory genes expressed asymmetrically during mouse development, and its absence results in LR axis malformations (Kitamura et al., 1999; Lin et al., 1999; Lu et al., 1999). Two of 15 *Zic3*-null embryos from four to 14 somites of development had abnormal *Pitx2* expression: one with diffuse left-sided expression and the other embryo with diffuse bilateral expression (head mesenchyme expression was normal in both) (Fig. 4F,G). All of the heterozygous and wild-type littermates had normal, left-sided expression (Fig. 4E).

Nodal is the earliest gene that is expressed asymmetrically during mouse development (Lowe et al., 1996). *Nodal* expression was studied using in situ hybridization in *Zic3* wild-type, heterozygous and null embryos ranging from presomite to eight somite stages (Fig. 4 and Table 3). In wild-type embryos, *nodal* expression is observed in the left LPM from the two- to eight-somite stage. Among *Zic3*-null embryos,

Table 2. Combination of LR patterning defects, CNS defects and axial skeletal patterning defects seen in *Zic3* null and heterozygous mice

		Left-Right						
			Lung					
Group	Number	Heart	Right	Left	Rev	Right stomach	CNS	Axial skeleton
A	8	8	3	2	3	3	–	–
B	3	2	1	–	1	1	3	–
C	6	4	4	–	–	1	–	6
D	3	3	1	–	–	1	3	3
E	2	–	–	–	–	–	2	–
F	2	–	–	–	–	–	–	2
G	1	–	–	–	–	–	1	1
Totals	25	17	9	2	4	6	9	12

–, no defect.

nodal expression appeared randomized in the sidedness of its LPM expression: three embryos expressed *nodal* on the left, three on the right and one bilaterally.

Nodal expression normally begins at the node earlier than in the LPM and persists longer (Collignon et al., 1996; Lowe et al., 1996). Unlike LPM expression, which often is not detected among wild-type embryos (presumably because of its brevity), expression at the node is always observed in embryos up to the six-somite stage. Correct *nodal* expression at the node appeared in *Zic3* heterozygotes and *Zic3*-null embryos up to the two-somite stage, but seven out of 16 heterozygote or null embryos from two to six somites lacked expression at the node, whereas all 14 wild-type embryos examined at this stage had correct *nodal* expression at the node (Fig. 4 and Table 3). At the six- to eight-somite stage, no *nodal* expression was detected in 6/7 heterozygote or null embryos compared with 1/3 wild-type embryos. Among the seven embryos with two to six somites with absent expression at the node, LPM expression was observed on the right side in three, on the left side in two, bilaterally in one and absent in one. Right-sided or bilateral LPM expression was always accompanied by absent expression at the node.

DISCUSSION

Zic3 null mice recapitulate laterality defects found in humans with HTX1

Laterality defects are a common (one in 8500 live births) and important cause of congenital malformations (Ferencz et al., 1997). Although several genes are known to affect laterality in various model organisms, the molecular basis for the majority of human cases is not known and generalizations across species have been difficult in some cases, owing to lack of conserved gene function. Our results indicate that *Zic3* null mice correctly model the defects seen in individuals with HTX1, particularly with regard to situs abnormalities and congenital heart defects, and will be an important model for investigating the mechanistic underpinnings of these disorders.

In the original HTX1 study, no phenotypically normal male offspring of carrier females were described (15 in total) (Gebbia et al., 1997). A later case report has documented a male with a mutation in *ZIC3* with no obvious malformations, although other male family members had characteristic HTX1 (Megarbane et al., 2000). In our mouse model, 80% of the *Zic3* null mice have phenotypic abnormalities that manifest either in the embryonic or perinatal period, with the remaining 20% apparently without obvious malformation with the exception of a 'kinked' tail. There is a subset of individuals with HTX1 in which the carriers show situs inversus. In the *Zic3* heterozygous females, laterality defects were detected in six out of 55 animals examined and included one case of situs inversus. These results indicate that both complete and partial deficiency of *Zic3* can cause disturbances of laterality. Genetic background appears to influence the penetrance of the phenotype with increased lethality noted on an inbred 129 background. The fact that some null animals survive to adulthood suggests that *Zic3* is not absolutely essential during development and implies a permissive role. Our finding that more *Zic3* null males died in utero, whereas more *Zic3* null females died in the perinatal period suggests a sex-limited effect that will require additional investigation. The majority

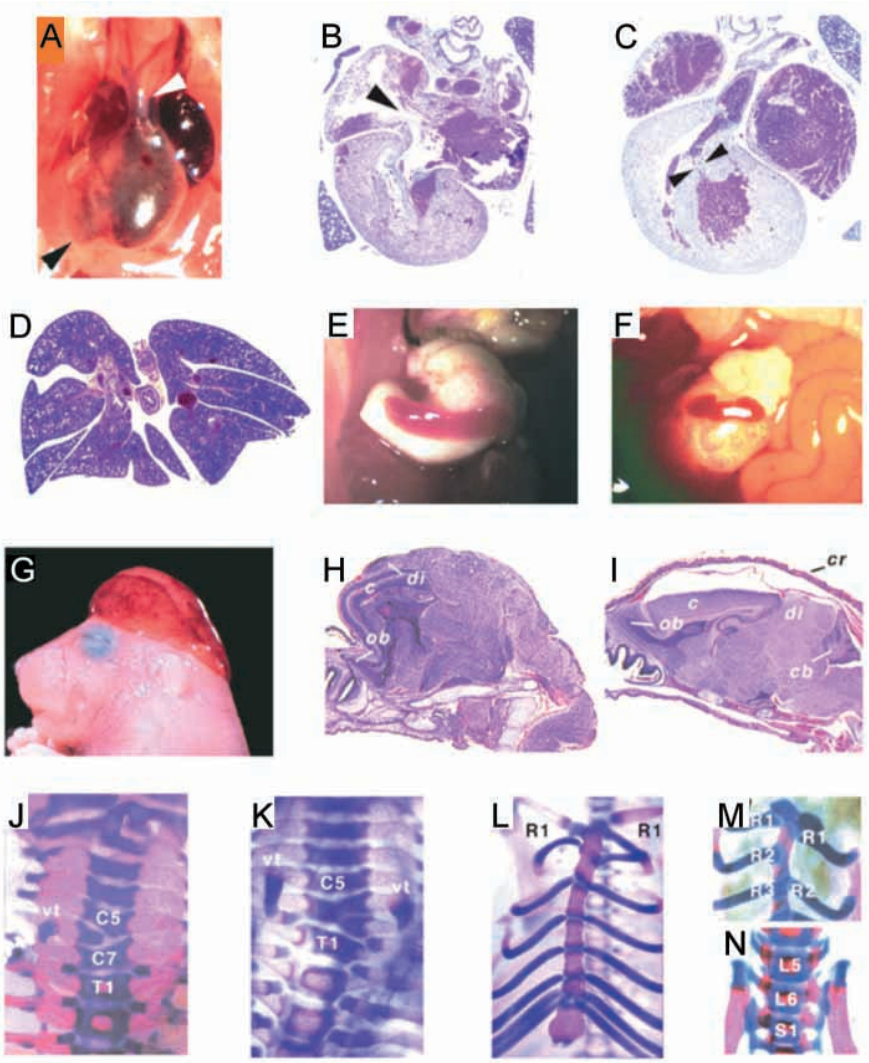

Fig. 3. Internal malformations in *Zic3*-null mice. (A) Dextrocardia (black arrowhead) and transposition of the great arteries [position of aorta (white arrowhead) anterior to pulmonary artery]. (B) Atrial septal defect (arrowhead) and (C) ventricular septal defect (between arrowheads). (D) Bilateral multilobate lungs characteristic of right pulmonary isomerism. (E,F) Normal (E) and hypoplastic (F) spleens in wild-type and null embryos, respectively. (G) Exencephaly. (H) Disorganized cortex (c); hypoplastic, disorganized olfactory bulb (ob); anteriorly displaced diencephalon (di) in exencephalic brain. When compared with wild-type brain in (I), note absence of cranium (cr) and cerebellum (cb). (J) Absence of left C6 hemivertebra. (K) Right ventral tubercle on C5 (normally on C6) and hemivertebrae deficiency on right (normally seven cervical vertebrae). (L) Partial duplication of left first rib. (M) Insertion of R2 in R3 position on left. (N) Left hemivertebra L6 has articular surface for ileum, a feature typical of S1.

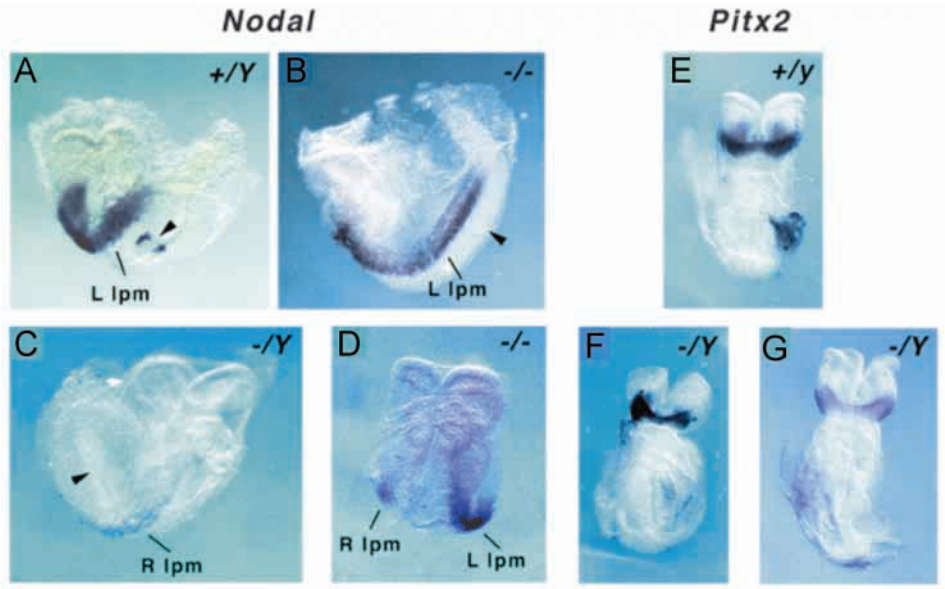

Fig. 4. *Nodal* and *Pitx2* expression in *Zic3* mutant embryos. Whole-mount in situ hybridization analysis of *Nodal* mRNA expression in 4-6 somite embryos (A-D) and *Pitx2* mRNA expression in 8-10 somite embryos (E-G). Embryos are oriented anterior towards the top and are viewed from the side (A,B; left of the figure is the left side of the embryo), posteriorly (C; right of the figure is the right side of the embryo) or the ventral side (D-G; right of the figure is the left side of the embryo). (A) Wild-type male showing left sided lateral plate mesoderm expression and expression at the node. (B) Null female showing left lateral plate mesoderm expression and absent nodal expression. (C) Null male showing right sided lateral plate mesoderm expression and absent nodal expression. (D) Null female showing bilateral lateral plate mesoderm expression, the expression being stronger on the left. Node expression was absent (not visible in this view). (E) Wild-type male showing the expected *Pitx2* left sided lateral plate mesoderm expression and expression in the head mesenchyme. (F) Null male showing ill-defined left sided expression and normal head mesenchyme expression. (G) Null male showing diffuse bilateral lateral plate mesoderm expression and normal head mesenchyme expression.

of perinatal deaths were attributable to CHD, suggesting that the null females may be more susceptible to this particular defect. Our results, together with those of others who have investigated laterality abnormalities in offspring of nonobese diabetic (NOD) mice (Maeyama et al., 2001) and in *cryptic*/EGF-CFC knockout mice (Bamford et al., 2000), indicate the role for environmental and/or genetic modifying loci in contributing to the laterality phenotype both in mice and in humans. Because the *Zic3* null mice are comparable with individuals with HTX1 in terms of the degree of affected offspring and carriers, they will be useful to begin investigations of contributing modifier loci.

Bent tail mice are deleted for the *Zic3* locus

Bent tail (*Bn*) is a spontaneous mutation of the X chromosome that has been used as a mouse model of neural tube defects (Garber, 1952). Mapping of the *Bn* crucial region demonstrated the mutation is associated with a submicroscopic deletion on the proximal part of the X chromosome, a region that includes the *Zic3* locus (Carrel et al., 2000; Klootwijk et al., 2000). Short 'kinked' tails characterize the mice. Abnormalities of thoracic situs and neural tube defects, including exencephaly, were noted in these animals. In addition, one report noted cleft lip, orofacial schisis and gastroschisis in a subset of *Bn* mice. The original description of the *Bn* mice described several with forelimb abnormalities. We have not found gastroschisis, orofacial clefting or forelimb abnormalities in any of the *Zic3* null or heterozygous mice examined to date. We cannot formally rule out the possibility that mice born with these defects died in the perinatal period and missed analysis. More likely possibilities include that the *Bn* deletion is a contiguous gene syndrome and that other genes within the submicroscopic

Table 3. *Nodal* expression pattern in *Zic3* null and heterozygous embryos

Somites	Node		Lateral plate mesoderm			
Stage and genotype	Present	Absent	Absent	Left	Bilateral	Right
0-2 somites						
Wild type	5		5			
Heterozygous	1					
Null	4		4			
2-4 somites						
Wild type	1		1			
Heterozygous						
Null	5	1	3	2		1
4-6 somites						
Wild type	13	4	9	4		
Heterozygous	4	2	3	3		
Null	1	4	1	1	1	2
6-8 somites						
Wild type	2	1	3			
Heterozygous	1	3	4			
Null		3	3			

deletion are responsible for these features. Alternatively, there may be a phenotypic variation in expression that is strain dependent and/or influenced by other loci. We conclude that deletion of *Zic3* contributes to the situs abnormalities and neural tube defects in the *Bn* tail mice, whereas the other noted anomalies in these mice appear to be unrelated to *Zic3* deficiency.

Deletion of *Zic3* causes defects of laterality, axial patterning and CNS development

In *Zic3* null and heterozygous mice, the situs abnormalities are similar to those found in humans. The non-LR malformations seen in humans (e.g. renal and anal) generally differ from those identified in mouse (exencephaly and skeletal) although olfactory nerve and cerebellar abnormalities have been observed in both mouse and human. Early pregnancy loss (prior to organogenesis in the mice and within the first trimester in humans) occurs in both humans (Casey et al., 1993) and *Zic3* null mice. Further analysis of *Zic3* null mice at early embryonic stages will be required to identify the cause(s) of this loss.

Murine lung anatomy is a readily identifiable marker of left-right asymmetry because the right lung normally has four lobes and the left lung has one lobe. Knockout mice have been described in which left pulmonary isomerism (one lobe bilaterally) or right pulmonary isomerism (four lobes bilaterally) is seen. Knockouts that show left pulmonary isomerism include *Shh* and *Lefty1* (Chiang et al., 1996; Meno et al., 1998). These genes are both hypothesized to play a role at the midline, restricting *Nodal*, *Lefty2* and *Pitx2* expression to the left LPM, thereby reinforcing the left identity. Loss of these genes results in bilateral expression of the LPM signaling cascade and bilateral left sidedness. Activin receptor IIB (Oh and Li, 1997), *cryptic*/EGF-CFC (Yan et al., 1999) and *Gdf1* (Rankin et al., 2000) knockouts, as well as *Fgf8* hypomorphs (Meyers and Martin, 1999), all demonstrate right pulmonary isomerism. These genes are hypothesized to act prior to or within the asymmetric cascade of gene expression within the left LPM. Loss of gene expression leads to absence of the left sided cascade and a right-sided identity develops, presumably as a default pathway. In *iv/iv* or *lrd* mice as well as *inv* mice, pulmonary reversal is the predominant phenotypic lung finding. Lung anatomy is therefore not only an indicator of asymmetry, but is also related to the site of action of a gene within the hierarchy of LR axis generation. The finding of both right and left pulmonary isomerism as well as pulmonary reversal in null *Zic3* mice is therefore mechanistically important. The pulmonary reversal indicates *Zic3* can exert an effect at the level of axis specification and/or orientation. By contrast, the finding of pulmonary isomerism indicates a role in the propagation of the lateralized signaling cascade. To our knowledge, this is the first gene involved in LR asymmetry in which both left and right pulmonary isomerism is seen.

In addition to laterality defects, *Zic3* mice also show defects of axial patterning and neural tube closure. In early *Zic3* deficient embryos, failure to turn or abnormal turning is noted, suggesting defective midline patterning. Several mouse models that produce both neural defects and a disruption of axial patterning, including *no turning* (Melloy et al., 1998) and *Sil* (Izraeli et al., 1999) mutants, as well as *Kif3a* (Marszalek et al., 1999; Takeda et al., 1999), *Kif3b* (Nonaka et al., 1998) and *Hnf3b* (Ang and Rossant, 1994; Weinstein et al., 1994) knockout mice, show a concomitant disruption of LR axis formation, suggesting that LR asymmetry and axial patterning can be linked. The axial patterning defects in *Zic3* mice are further emphasized by the skeletal abnormalities, which occur in ribs and vertebrae, both derivatives of the dorsal sclerotome. Deficiency of *Zic3* also results in a bent tail, presumably caused, as in the *Bn* mice, by asymmetric growth of caudal vertebrae (Klootwijk et al., 2000). Therefore, lack of *Zic3* appears to perturb both anteroposterior and LR patterning during embryonic development.

Previous studies in *Zic1*-deficient mice and *Zic2* knockdown mice have demonstrated skeletal and CNS anomalies. The skeletal findings in *Zic1* null mice are very similar to those noted here, whereas the *Zic2* mice have limb anomalies in addition to vertebral anomalies. Humans with *ZIC2* mutations have holoprosencephaly, a defect also seen in the knockdown mice together with exencephaly, anencephaly and spina bifida (Brown et al., 1998; Nagai et al., 2000). *Zic1* null mice demonstrated cerebellar dysgenesis (Aruga et al., 1998). Several studies have shown significant Zic-Gli interaction in neural and skeletal patterning, and Zic and Gli proteins have been shown to physically and functionally interact through their zinc-finger domains (Koyabu et al., 2001). This interaction may be synergistic, as in the double mutation of *Zic1* and *Gli3* which results in increased disturbance of segmentation of the vertebral lamina (Aruga et al., 1999), or it may be inhibitory, as in the case of the Zic2-Gli2 interaction in the patterning of the neural tube along the dorsoventral axis in *Xenopus* (Brewster et al., 1998). The nature of Zic-Gli interactions are only beginning to be characterized and it will be important to consider them in a developmental stage specific and cell type specific context. It is currently unclear to what degree other *Zic* family members can compensate for *Zic3* deficiency although there is precedent from the *Gli2* and *Gli3* knockout mice for both specific individual functions as well as redundant functions in skeletal patterning.

The role of *Zic3* in axis specification and maintenance of asymmetric signals

The generation of LR asymmetry requires LR axis specification, orientation with respect to the dorsoventral and anteroposterior axes, and propagation of asymmetric LR signals. Our results indicate that *Zic3* functions at the node and in the midline and participates both in LR axis specification and maintenance of asymmetric signaling in the left LPM. *Zic3*-deficient embryos fail to maintain *Nodal* expression after the two somite stage and exhibit randomized expression of *Nodal* and *Pitx2* in the LPM, placing *Zic3* upstream of these genes within the left-right specification pathway. In contrast to our results, *Fgf8* neo/- hypomorphic embryos fail to express *Nodal* at the node at the zero- to two-somite stage, suggesting a defect in the initiation of *nodal* expression (Meyers and Martin, 1999). Taken together, these results appear to place *Zic3* between *Fgf8* and LPM *Nodal* in the left-right pathway. In addition, *Zic3* appears to be important in the specification of LR asymmetry based on the finding of situs inversus as well as pulmonary reversal in a subset of *Zic3*-deficient mice. The requirement for *Zic3* in the midline is demonstrated by the axial patterning defects in the null mice as well as pulmonary isomerism. Further investigation of midline defects in these

mice, including molecular characterization, will be required to determine whether this represents a primary process or is secondary to abnormalities within the node.

Gli proteins are important mediators of *Shh* signals that are involved in LR, CNS and somite patterning. In vitro data have shown that Zic proteins are relatively weak transcriptional activators and may function instead as transcriptional coactivators with Gli proteins (Mizugishi et al., 2001). Based on the known functional interactions between Gli and Zic proteins (Koyabu et al., 2001), the function of *Zic3* may be modulated by *Shh* or via interactions with combinations of Gli-family transcription factors downstream of *Shh* signaling. Furthermore, *Gli2* is induced by FGF signaling in *Xenopus*. It is therefore tempting to speculate that *Zic3* acts in concert with Gli-family transcription factors to establish a midline developmental field required for enforcement of left and right identities via its interaction with FGF8 (responsible for left identity) and *Shh* (responsible for restricting left). Thus, *Zic3* would be permissive but not sufficient for LR axis determination, and deficiency could result in left isomerism, right isomerism or reversal, based on the balance of competing left and right signals.

In summary, *Zic3* is important in the development of left-right asymmetry and may function at multiple levels within this pathway, acting both at the node, in order to maintain *Nodal* expression, and in the midline. Its deficiency results in prenatal lethality in approximately 50% of mice and defects in laterality, axial patterning and neural tube formation are seen, suggestive of an important role of *Zic3* in early mesodermal patterning. The phenotypes seen in *Zic3* null mice are similar to those found in human HTX1 and these mice will be useful in studies to delineate the molecular mechanisms underlying the variable effects of mutation at this locus.

We thank Allan Bradley for the mouse ES and STO cell lines. This work was supported in part by grants from the March of Dimes (1-FY98-0310 to B. C.), the American Heart Association (#96015660 to B. C.) and the NIH (K08 HD01078 to B. C., K08 HL67355 to S. M. W. and PO1 HL67155 to J. W. B.). Veterinary resources at the M. D. Anderson Cancer Center were supported by the Cancer Center Support (Core) Grant (CA16672).

REFERENCES

Ang, S.-L. and Rossant, J. (1994). HNF-3β is essential for node and notochord formation in mouse development. *Cell* **78**, 561-574.

Aruga, J., Yokota, N., Hashimoto, M., Furuichi, T., Fukuda, M. and Mikoshiba, K. (1994). A novel zinc finger protein, Zic, is involved in neurogenesis, especially in the cell lineage of cerebellar granule cells. *J. Neurochem*. **63**, 1880-1890.

Aruga, J., Nagai, T., Tokuyama, T., Hayashizaki, Y., Okazaki, Y., Chapman, V. M. and Mikoshiba, K. (1996a). The mouse *Zic* gene family. *J. Biol. Chem*. **271**, 1043-1047.

Aruga, J., Yozu, A., Hayashizaki, Y., Okazaki, Y., Chapman, M. M. and Mikoshiba, K. (1996b). Identification and characterization of *Zic4*, a new member of the mouse *Zic* gene family. *Gene* **172**, 291-294.

Aruga, J., Minowa, O., Yaginuma, H., Kuno, J., Nagai, T., Noda, T. and Mikoshiba, K. (1998). Mouse *Zic1* is involved in cerebellar development. *J. Neurosci.* **18**, 284-293.

Aruga, J., Mizugishi, K., Koseki, H., Imai, K., Balling, R., Noda, T. and Mikoshiba, K. (1999). *Zic1* regulates the patterning of vertebral arches in cooperation with *Gli3*. *Mech. Dev.* **89**, 141-150.

Bamford, R. N., Roessler, E., Burdine, R. D., Saplakoglu, U., de la Cruz, J., Splitt, M., Goodship, J. A., Towbin, J., Bowers, P., Ferrero, G. B. et al. (2000). Loss-of-function mutations in the EGF-CFC gene CFC1 are associated with human left-right laterality defects. *Nat. Genet.* **26**, 365-369.

Behringer, R. R., Finegold, M. J. and Cate, R. L. (1994). Mullerian-inhibiting substance function during mammalian sexual development. *Cell* **79,** 415-425.

Brewster, R., Lee, J. and Ruiz i Altaba, A. (1998). Gli/Zic factors pattern the neural plate by defining domains of cell differentiation. *Nature* **393**, 579-583.

Brown, S. A., Warburton, D., Brown, L. Y., Yu, C. Y., Roeder, E. R., Stengel-Rutkowski, S., Hennekam, R. C. and Muenke, M. (1998). Holoprosencephaly due to mutations in ZIC2, a homologue of Drosophila odd-paired. *Nat. Genet.* **20**, 180-183.

Burdine, R. D. and Schier, A. F. (2000). Conserved and divergent mechanisms in left-right axis formation. *Genes Dev.* **14**, 763-776.

Campione, M., Steinbeisser, H., Schweickert, A., Deissler, K., van Bebber, F., Lowe, L. A., Nowotschin, S., Viebahn, C., Haffter, P., Kuehn, M. R. and Blum, M. (1999). The homeobox gene Pitx2: mediator of asymmetric left-right signaling in vertebrate heart and gut looping. *Development* **125**, 1225-1234.

Capdevila, J., Vogan K. J., Tabin C. J. and Izpisua-Belmonte J. C. (2000). Mechanisms of left-right determination in vertebrates. *Cell* **101**, 9-21.

Carrel, T., Purandare, S. M., Harrison, W., Elder, F., Fox, T., Casey, B. and Herman, G. E. (2000). The X-linked mouse mutation Bent tail is associated with a deletion of the *Zic3* locus. *Hum. Mol. Genet.* **9**, 1937-1942.

Casey, B., Devoto, M., Jones, K. L. and Ballabio, A. (1993). Mapping a gene for familial situs abnormalities to human chromosome Xq24-q27.1. *Nat. Genet*. **5**, 403-407.

Casey, B. and Hackett, B. P. (2000). Left-right axis malformations in man and mouse. *Curr. Opin. Genet. Dev.* **10**, 257-261.

Chen, J., Knowles, H. J., Hebert, J. L. and Hackett, B. P. (1998). Mutation of the mouse hepatocyte nuclear factor/forkhead homologue 4 gene results in an absence of cilia and random left-right asymmetry. *J. Clin. Invest.* **102**, 1077-1082.

Chiang, C., Litingtung, Y., Lee, E., Young, K. E., Corden, J. L., Westphal, H. and Beachy, P. A. (1996). Cyclopia and defective axial patterning in mice lacking *Sonic hedgehog* gene function. *Nature* **383**, 407-413.

Collignon, J., Varlet, I. and Robertson, E. J. (1996). Relationship between asymmetric *nodal* expression and the direction of embryonic turning. *Nature* **381**, 155-158.

Ferencz, C., Loffredo, C., Correa-Villasenor, A. and Wilson, P. (1997). Genetic and environmental risk factors of major cardiovascular malformations: The Baltimore-Washington infant study 1981-1989. Armonk, NY: Futura Press.

Garber, E. D. (1952). Bent tail, a dominant, sex-linked mutation in the mouse. *Proc. Natl. Acad. Sci. USA* **38**, 876-879.

Gebbia, M., Ferrero, G. B., Pilia, G., Bassi, M. T., Aylsworth, A. S., Penman-Splitt, M., Bird, L. M., Bamforth, J. S., Burn, J., Schlessinger, D. et al. (1997). X-linked situs abnormalities result from mutations in ZIC3. *Nat. Genet*. **17**, 305-308.

Harvey, R. P. (1998). Links in the left-right axial pathway. *Cell* **94**, 273-276.

Hogan, B., Beddington, R., Constantini, F. and Lacey, E. (1994). Manipulating the mouse embryo. Plainview: Cold Spring Harbor Press.

Hummel, K. P. and Chapman, D. B. (1959). Visceral inversion and associated anomalies in the mouse. *J. Hered.* **50**, 9-13.

Izraeli, S., Lowe, L. A., Bertness, V., Good, D. J., Dorward, D. W., Kirsch, I. R. and Kuehn, M. R. (1999). The SIL gene is required for mouse embryonic axial development and left-right specification. *Nature* **399**, 691-694.

Kitaguchi, T., Nagai, T., Nakata, K., Aruga, J. and Mikoshiba, K. (2000). *Zic3* is involved in the left-right specification of the *Xenopus* embryo. *Development* **127**, 4787-4795.

Kitamura, K., Miura, H., Miyagawa-Tomita, S., Yanazawa, M., Katoh-Fukui, Y., Suzuki, R., Ohuchi, H., Suehiro, A., Motegi, Y., Nakahara, Y. et al. (1999). Mouse *Pitx2* deficiency leads to anomalies of the ventral body wall, heart, extra- and periocular mesoderm and right pulmonary isomerism. *Development* **126**, 5749-5758.

Klootwijk, R., Franke, B., van der Zee, C. E., de Boer, R. T., Wilms, W., Hol, F. A. and Mariman, E. C. (2000). A deletion encompassing *Zic3* in bent tail, a mouse model for X-linked neural tube defects. *Hum. Mol. Genet.* **9**, 1615-1622.

Kochhar, D. M. (1973). Limb development in mouse embryos. Analysis of teratogenic effects of retinoic acid. *Teratology* **7**, 289-298.

Koyabu, Y., Nakata, K., Mizugishi, K., Aruga, J. and Mikoshiba, K.

(2001). Physical and functional interactions between Zic and Gli proteins. *J. Biol. Chem.* **276**, 6889-6892.

Lin, C. R., Kioussi, C., O'Connel, S., Briata, P., Szeto D., Liu, F., Izpisua-Belmonte, J. C. and Rosenfeld, M. G. (1999). Pitx2 regulates lung asymmetry, cardiac positioning and pituitary and tooth morphogenesis. *Nature* **401**, 279-282.

Lin, J. C. and Cepko, C. L. (1998). Granule cell raphes and parasagittal domains of Purkinje cells: complementary patterns in the developing chick cerebellum. *J. Neurosci.* **18**, 9342-9353.

Logan, M., Pagan-Westphal, S. M., Smith, D. M., Paganessi, L. and Tabin, C. J. (1998). The transcription factor Pitx2 mediates situs-specific morphogenesis in response to left-right asymmetric signals. *Cell* **94**, 307-317.

Lowe, L. A., Supp, D. M., Sampath, K., Yokoyama, T., Wright, C. V. E., Potter, S. S., Overbeek, P. and Kuehn, M. R. (1996). Conserved left-right asymmetry of nodal expression and alterations in murine *situs inversus. Nature* **381**, 158-161.

Lu, M. F., Pressman, C., Dyer, R., Johnson, R. L. and Martin, J. F. (1999). Function of Rieger syndrome gene in left-right asymmetry and craniofacial development. *Nature* **401**, 276-278.

Maeyama, K., Kosaki, R., Yoshihashi, H., Casey, B. and Kosaki, K. (2001). Mutation analysis of left-right axis determining genes in NOD and ICR, strains susceptible to maternal diabetes. *Teratology* **63**, 119-126.

Mansour, S., Thomas, K. and Capecchi, M. (1988). Disruption of the proto-oncogene int-2 in mouse embryo-derived stem cells: a general stategy for targeting mutations to non-selectable genes. *Nature* **336**, 348-352.

Marszalek, J. R., Ruiz-Lozano, P., Roberts, E., Chien, K. R. and Goldstein, L. S. B. (1999). Situs inversus and embryonic ciliary morphogenesis defects in mouse mutants lacking the KIF3A subunit of kinesin-II. *Proc. Natl. Acad. Sci. USA* **96**, 5043-5048.

Megarbane, A., Salem, N., Stephan, E., Ashoush, R., Lenoir, D., Delague, V., Kassab, R., Loiselet, J. and Bouvagnet, P. (2000). X-linked transposition of the great arteries and incomplete penetrance among males with a nonsense mutation in *ZIC3*. *Eur. J. Hum. Genet*. **8**, 704-708.

Melloy, P. G., Ewart, J. L., Cohen, M. F., Desmond, M. E., Kuehn, M. R. and Lo, C. W. (1998). *No turning*, a mouse mutation causing left-right and axial patterning defects. *Dev. Biol*. **193**, 77-89.

Meno, C., Saijoh, Y., Fujii, H., Ikeda, M., Yokoyama, T., Yokoyama, M., Toyoda, Y. and Hamada, H. (1996). Left-right asymmetric expression of the TGFβ-family member *lefty* in mouse embryos. *Nature* **381**, 151-155.

Meno, C., Shimono, A., Saijoh, Y., Yashiro, K., Mochida, K., Ohishi, S., Noji, S., Kondoh, H. and Hamada, H. (1998). Lefty-1 is required for left-right determination as a regulator of lefty-2 and nodal. *Cell* **94**, 287-297.

Meno, C., Gritsman, K., Ohishi, S., Ohfuji, Y., Heckscher, E., Mochida, K., Shimono, A., Kondoh, H., Talbot, W. S., Robertson, E. J. et al. (1999). Mouse lefty2 and zebrafish antivin are feedback inhibitors of nodal signaling during vertebrate gastrulation. *Mol. Cell*. **4**, 287-298.

Meyers, E. N. and Martin, G. R. (1999). Differences in left-right axis pathways in mouse and chick: functions of FGF8 and SHH. *Science* **285**, 403-406.

Mizugishi, K., Aruga, J., Nakata, K. and Mikoshiba, K. (2001). Molecular properties of Zic proteins as transcriptional regulators and their relationship to GLI proteins. *J. Biol. Chem.* **276**, 2180-2188.

Mochizuki, T., Saijoh, Y., Tsuchiya, K., Shirayoshi, Y., Takai, S., Taya, C., Yonekawa, H., Yamada, K., Nihei, H., Nakatsuji, N. et al. (1998). Cloning of *inv*, a gene that controls left/right asymmetry and kidney development. *Nature* **395**, 177-181.

Nagai, T., Aruga, J., Takada, S., Gunther, T., Sporle, R., Schughart, K. and Mikoshiba, K. (1997). The expression of the mouse *Zic1, Zic2, and Zic3* gene suggests an essential role for *Zic* genes in body pattern formation. *Dev. Biol*. **182**, 299-313.

Nagai, T., Aruga, J., Minowa, O., Sugimoto, T., Ohno, Y., Noda, T. and Mikoshiba, K. (2000). Zic2 regulates the kinetics of neurulation. *Proc. Natl. Acad. Sci. USA* **97**, 1618-1623.

Nakata, K., Nagai, T., Aruga, J. and Mikoshiba, K. (1997). *Xenopus Zic3*, a primary regulator both in neural and neural crest development. *Proc. Natl. Acad. Sci. USA* **94**, 11980-11985.

Nakata, K., Koyabu, Y., Aruga, J. and Mikoshiba, K. (2000). A novel member of the *Xenopus Zic* family, *Zic5*, mediates neural crest development. *Mech. Dev.* **99**, 83-91.

Nonaka, S., Tanaka, Y., Okada, Y., Takeda, S., Harada, A., Kanai, Y., Kido, M. and Hirokawa, N. (1999). Randomization of left-right asymmetry due to loss of nodal cilia generating leftward flow of extraembryonic fluid in mice lacking KIF3B motor protein. *Cell* **95**, 829-837.

Oh, S. P. and Li, E. (1997). The signaling pathway mediated by the type IIB activin receptor controls axial patterning and lateral asymmetry in the mouse. *Genes Dev.* **11**, 1812-1826.

Piedra, M. E., Icardo, J. M., Albajar, M., Rodriguez-Rey, J. C. and Ros, M. A. (1998). *Pitx2* participates in the late phase of the pathway controlling left-right asymmetry. *Cell* **94**, 319-324.

Rankin, C. T., Bunton, T., Lawler, A. M. and Lee, S.-J. (2000). Regulation of left-right patterning in mice by growth/differentiation factor-1. *Nat. Genet.* **24**, 262-265.

Ryan, A. K., Blumberg, B., Rodriguez-Esteban, C., Yonei-Tamura, S., Tamura, K., Tsukui, T., de la Pena, J., Sabbagh, W., Greenwald, J., Choe, S. et al. (1998). Pitx2 determines left-right asymmetry of internal organs in vertebrates. *Nature* **394**, 545-551.

Supp, D. M., Witte, D. P., Potter, S. S. and Brueckner M. (1997). Mutation of an axonemal dynein affects left-right asymmetry in *inversus viscerum* mice. *Nature* **389**, 963-966.

Supp, D. M., Brueckner, M., Kuehn, M. R., Witte, D. P., Lowe, L. A., McGrath, J., Corrales, J. and Potter, S. S. (1999). Targeted deletion of the ATP binding domain of left-right dynein confirms its role in specifying development of left-right asymmetries. *Development* **126**, 5495-5504.

Takeda, S., Yonekawa, Y., Tanaka, Y., Okada, Y., Nonaka, S. and Nobutaka, H. (1999). Left-right asymmetry and kinesin superfamily protein KIF3A: new insights in determination of laterality and mesoderm induction by *kif3A*$^{-/-}$ mice analysis. *J. Cell Biol*. **145**, 825-836.

Tsukui, T., Capdevila, J., Tamura, K., Ruiz-Lozano, P., Rodriguez-Esteban, C., Yonei-Tamura, S., Magallon, J., Chandraratna, R. A. S., Chien, K., Blumberg, B. et al. (1999). Multiple left-right asymmetry defects in *Shh*$^{-/-}$ mutant mice unveil a convergence of the Shh and retinoic acid pathways in the control of *Lefty-1*. *Proc. Natl. Acad. Sci. USA* **96**, 11376-11381.

Weinstein, D. C., Ruiz i Altaba, A., Chen, W. S., Hoodless, P., Prezioso, V. R., Jessell, T. M. and Darnell, J. E. (1994). The winged helix transcription factor HNF-3β is required for notochord development in the mouse embryo. *Cell* **78**, 575-588.

Wilkinson, D. G. (1992). In Situ *Hybridization: A Practical Approach*. London, UK: Oxford University Press.

Yan, Y.-R., Gritsman, K., Ding, J., Burdine, R. D., Corrales, J. D., Price, S. M., Talbot, W. S., Schier, A. F. and Shen, M. M. (1999). Conserved requirement for *EGF-CFC* genes in vertebrate left-right axis formation. *Genes Dev.* **13**, 2527-2537.

Yokoyama, T., Copeland, N. G., Jenkins, N. A., Mongomery, C. A., Elder, F. F. B. and Overbeek, P. A. (1993). Reversal of left-right asymmetry: a situs inversus mutation. *Science* **260**, 679-682.

Yoshioka, H., Meno, C., Koshiba, K., Sugihara, M., Itoh, H., Ishimaru, Y., Inoue, T., Ohuchi, H., Semina, E. V., Murray, J. C., Hamada, H. and Noji, S. (1998). *Pitx2*, a bicoid-type homeobox gene, is involved in a lefty-signaling pathway in determination of left-right asymmetry. *Cell* **94**, 299-305.